frontiers | Frontiers in Energy Research

TYPE Original Research
PUBLISHED 07 March 2024
DOI 10.3389/fenrg.2024.1308519

OPEN ACCESS

EDITED BY
Ellen B. Stechel,
Arizona State University, United States

REVIEWED BY
Vedran Mrzljak,
University of Rijeka, Croatia
Zhiqing Zhang,
Guangxi University of Technology, China

*CORRESPONDENCE
Lu Liang,
✉ lianglu@st.gxu.edu.cn

RECEIVED 06 October 2023
ACCEPTED 01 February 2024
PUBLISHED 07 March 2024

CITATION
Wang Z, Guan W, Zhang S, Sang H, Que W and Liang L (2024), Multi-objective optimization of the organic Rankine cycle cascade refrigeration cycle driven by sugar mills waste heat.
Front. Energy Res. 12:1308519.
doi: 10.3389/fenrg.2024.1308519

Multi-objective optimization of the organic Rankine cycle cascade refrigeration cycle driven by sugar mills waste heat

Zongrun Wang[1], Wei Guan[2], Song Zhang[3], Hailang Sang[3], Wenshuai Que[1] and Lu Liang[4]*

[1]Guangxi Key Laboratory of Manufacturing System and Advanced Manufacturing Technology, School of Mechanical Engineering, Guangxi University, Nanning, China, [2]Guangxi Key Laboratory of Petrochemical Resource Processing and Process Intensification Technology, Guangxi University, Nanning, China, [3]Advanced Technology Center, Research and Engineering Institute, Guangxi Yuchai Machinery Co., Ltd., Yulin, China, [4]College of Electrical Engineering Guangxi University, Nanning, China

The research on the recovery of low-grade thermal energy carried away by boiler flue gas is significant for sugar mills. This paper designs a waste heat recovery system based on sugar plant flue gas, integrating absorption refrigeration cycle and the organic Rankine cycle, and the effects of nine working fluids on the system are investigated. The aim is to realize the multi-form conversion of energy. The performance of the system is evaluated in terms of energy, exergy, and economic metrics. Multi-objective optimization is performed with the method of the NSGA-II genetic algorithm. The results show that Butane is the most suitable working fluid for ORC. The exergy efficiency of the system is 32.125% before optimisation, with an increased space cooling capacity of 15820.56 MW per year for the sugar mill. The exergy destruction analysis of the system reveals that the generator accounts for the highest proportion of exergy destruction (50.8%). The entire system shows the *LCOE* is as low as 0.0406$/kWh under the optimized condition. The optimized system can obtain an estimated annual electricity sales revenue of $136,300, and the sugar mill can save $308,600 in cooling costs. In addition, the payback period can be shortened to 5.79 years.

KEYWORDS

sugar mill, waste heat recovery, thermodynamic analysis, economic analysis, multi-objective optimization

1 Introduction

1.1 Background

Bioenergy is a large-scale renewable energy source, accounting for 10%–14% of the world's primary energy and potentially reaching 30%–40% by 2050 (Rosillo-Calle, 2016). Currently, over 120 million tons of sugar are produced worldwide each year, with approximately 70% derived from sugarcane (USDA, 2018). The biomass potential of this crop can replace fossil fuels, leading to energy savings (de Matos et al., 2020) and transforming the sugar industry into a more versatile and competitive sector. The untapped waste heat resources in the global sugar industry show great potential. In the production process of sugar mills, a large amount of sugarcane residue, such as bagasse are produced while a substantial amount of recoverable low-temperature waste heat are generated (Birru et al., 2016), making the recovery of waste heat emissions from sugar mills becomes very essential. Mohammadi et al. (2020) investigated the potential of using bagasse as a substitute for natural gas in a sugar factory for the generation of thermal energy and electricity. Singh (2019) analyzed the thermodynamic performance of a 16-megawatt cogeneration system in a sugar mill and found that 6.342% of the fuel energy was lost in the boiler flue gas. The substantial amount of low-temperature flue gas emitted by sugar mill boilers represents the main portion of heat loss and contains a significant amount of unused low-temperature waste heat. This not only affects the thermal efficiency of the boilers but also imposes significant pressure on the environment, causing ecological damage and contributing to intensified greenhouse effects. Fujii et al. (2019) demonstrated that the high-temperature flue gases produced from sugarcane boilers at approximately 200°C during the combustion process has been wasted, which could reduce fuel consumption by 29.6% if this portion of energy was effectively utilized. The aforementioned studies indicate that the boiler flue gases from sugar mills have not only high economic benefits, but also considerable thermodynamic potential.

1.2 Waste heat recovery technology of sugar factories

Organic Rankine cycle (ORC) system is more prominent in recovering low-temperature waste heat (Mana et al., 2023). ORC system not only converts waste heat into high-grade energy (electricity), but also are widely used due to their simplicity of construction, lower material and sealing costs, and adaptability to heat sources of different temperature levels (Nemati et al., 2017). Zhang et al. (2016) investigated the system properties of organic Rankine cycle (ORC), steam-organic Rankine cycle (S-ORC) as well as steam Rankine cycle (SRC) within the range of 150°C–350 °C by comparing their performances. The results indicated that more prominent thermodynamic performance and power generation are obtained when ORC is employed in the heat source temperature range of 150°C–210°C. Waste heat can be used for refrigeration in addition to electricity generation. Uphade (2021) studied the heat recovery potential of flue gas in the sugar industry and used a vapor absorption cycle instead of the conventional vapor compression cycle, allowing a sugar mill with 2,500 Tons of cane crushed per day capacity to produce 293 Tons of refrigeration cooling, which is sufficient to meet the internal demand of the sugar mill. Singh (2020) recovered waste heat from the boiler flue gases of the sugar mill, resulting in an increase of 375.2135 kW in the net power generation and an increase in the energy efficiency of the sugar mill's cogeneration by 0.3819%. Sugar mills need to consume huge financial and material resources in refrigeration every year (Du et al., 2014; Kapanji et al., 2021). In many heat-driven refrigeration systems, the absorption refrigeration technology is gradually becoming an effective alternative to the conventional vapor compression refrigeration system (Kumar et al., 2018) and is widely used in an increasing number of plants. This is due to its ability in fully utilizing low temperature heat sources to provide cooling capacity and the use of more eco-friendly refrigerants than chlorofluorocarbon refrigerants (CFCs) (Li et al., 2016). Bandgar al (Bandgar et al., 2018). utilized a vapor absorption system for waste heat recovery of excess water removed from the sugar mill for using as cooling in the factory office area. It saved 64,314 kWh per crushing season for the plant, which is equivalent to at least Rs. 529,304.22 per season. Chouhan and Chandrakar (2014) suggested the use of the absorption refrigeration system to recover heat sources, including flue gas and boiler emissions, which could save 1,870 tons of bagasse per year in terms of additional cooling capacity for sugar mills.

The separate utilization of ORC and absorption refrigeration has achieved excellent comprehensive benefits in various fields, but the energy generated by individual systems is relatively homogeneous in form and may not be as efficient as an integrated system. Therefore, some researchers have proposed cogeneration systems that integrate waste heat recovery technologies to upgrade the economic efficiency as well as the thermodynamic performance of the system and enrich forms of energy utilization. Dogbe et al. (2019) used absorption heat pump (AHP) technologies as well as organic Rankine cycle (ORC) to improve the energy efficiency in a sugar mill, resulting in a 1.7% improvement in exergy performance and a total bagasse value saving of 0.83%. Zhang et al. (2020) proposed a novel cogeneration system for coal-fired power plants based on ORC as well as AHP and evaluated the thermodynamic as well as economic efficiency of the system. The findings demonstrated that the power generation and heat production were increased by a factor of one, while the general exergy efficiency as well as thermal efficiency were increased by 9.38% and 1.71%, respectively, compared with the conventional CHP system. Wang et al. (2020) designed a new triple generation system consisting of an organic Rankine cycle, an absorption refrigeration cycle as well as a supercritical CO_2 Brayton cycle for waste heat recovery from gas turbines in addition. The results showed that the new system could produce 6.02 MW of cooling capacity, 9.93 MW of heat load, as well as 40.65 MW of net power generation. Tian et al. (2018) used an integrated system to increase system efficiency with a newly proposed triple system of CO_2 capture system, ammonia absorption cooler as well as organic Rankine cycle (ORC) integrated with SOFC. The calculation indicated that the exergy efficiency as well as net electrical efficiency of the comprehensive system can reach 59.96% and 52.83%, respectively.

1.3 Motivation and contribution

Currently, there is relatively little research on the construction and optimization of waste heat recovery systems in sugar factories, with most studies focused on cogeneration and single systems. In order to provide both electric and cooling power, and achieve efficient energy utilization, this study adopts the cascade Organic Rankine Cycle (ORC) and Absorption Refrigeration Cycle (ARC) waste heat recovery system. Sugar factories require a certain cooling system during sugar processing to control process temperatures, ensuring product quality and normal equipment operation, such as crystalline sugar particles and sugar storage. Therefore, using ORC-ARC to achieve combined cooling and power has significant significance. First, the ORC system is suitable for medium and low temperature waste heat recovery, with lower cost and simpler operation compared to other systems, such as reheating, reheat, and bypass. The ARC uses an absorbent to absorb and desorb the solute for cooling, and steam refrigeration cycles require compressors to compress steam, consuming more energy. At the same time, the absorbent used by ARC is more environmentally friendly than traditional refrigerants such as fluorine. Furthermore, both the

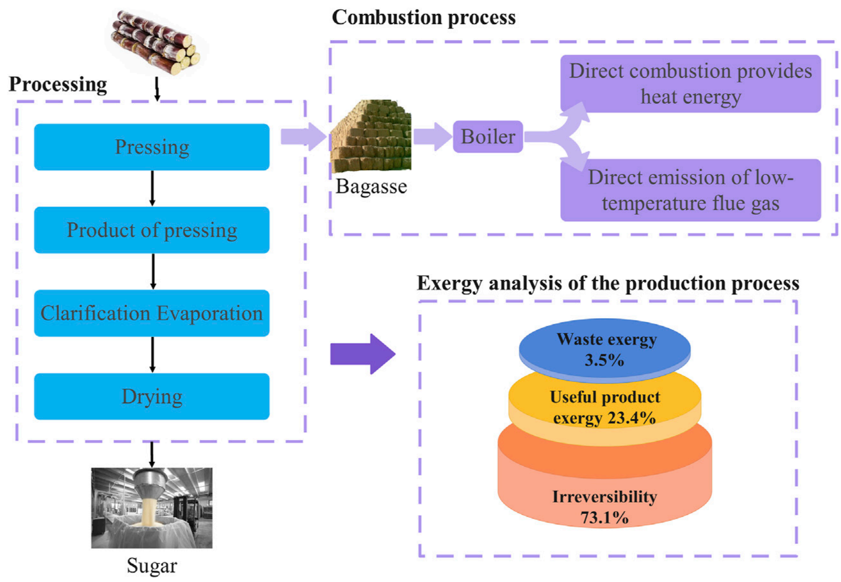

FIGURE 1
Process flow of sugar mill.

ORC and ARC systems possess high flexibility, allowing for efficient energy conversion by adjusting system parameters according to the requirements of the heat source and environment. Finally, by cascading ORC and ARC systems, not only can a large amount of "green" electricity be generated, but also sufficient cooling capacity provided for sugar factories, achieving efficient energy utilization and comprehensive recycling. Therefore, adopting the ORC-ARC system provides a feasible solution for waste heat recovery in sugar factories with higher economic and environmental performance.

This study compares the performance and environmental friendliness of nine working fluids in the ORC system, and determines the best organic working fluid in the integrated system based on comprehensive performance comparison, which helps optimize the operation of the entire integrated system. The performance of the ORC and absorption refrigeration cycle after integration is evaluated through thermodynamics and economic analysis, and the influence of key operating parameters such as evaporator temperature and generator temperature on the entire waste heat recovery system is studied. The economic efficiency of the system is evaluated using *LCOE*. Finally, NSGA-II is used to determine the system's optimal operating environment.

2 System description and assumptions

In this study, a new waste heat recovery system based on the flue gas of boilers in sugar mills is proposed. A specific analysis of the exergy in sugar mills has been carried out in the literature (Dogbe et al., 2018), and it was found that only 23.4% of the exergy in sugar mills leaves through the product during the whole production process, in which 3.5% of exergy is lost through waste and 73.1% is wasted during the production process due to various irreversible factors. The production process of a sugar mill is shown in Figure 1.

The significant energy loss caused by the waste heat from boiler flue gas during the production process can be effectively reduced by recovering this waste heat, thereby improving the economic performance and energy efficiency of the sugar factory. Considering that the recovered waste heat is around 190°C, an Organic Rankine Cycle (ORC) is used as the base cycle. Conventional steam refrigeration cycles require higher temperatures and pressures, making them less suitable for handling low-temperature waste heat (Li et al., 2014). ORC utilizes organic working fluids that can evaporate and condense at relatively low temperatures, making it particularly suitable for recovering low-temperature waste heat. Additionally, the Absorption Refrigeration Cycle (ARC) replaces traditional refrigerants with organic working fluids, which usually have minimal negative impact on the atmosphere. When the flue gas passes through the first round of energy recovery in the ORC, its temperature drops to a range suitable for capturing and utilizing by ARC, providing the sugar factory with additional refrigeration capacity. There are various areas in the sugar factory that require significant cooling, such as syrup cooling and crystallization cooling. By combining ORC with ARC, the waste heat from the boiler flue gas can be fully utilized. This not only converts waste heat into electrical energy but also provides additional refrigeration capacity, thereby improving the overall system performance and efficiency. The sugar factory can achieve efficient energy utilization, reduce energy consumption and emissions, and lower production costs. This is not only economically beneficial for the sugar factory itself but also aligns with environmental protection and sustainable development requirements. This research has achieved gradient utilization of boiler flue gas from sugar mills by integrating ORC and ARC, enabling multiform conversion of energy to cooling and electricity.

Figure 2 illustrates a schematic diagram of the complete waste heat recovery system. The principal components of the proposed system are the evaporator, condenser, turbine, absorber, pump, solution heat exchanger, and generator. The work process is: In the ORC system, the

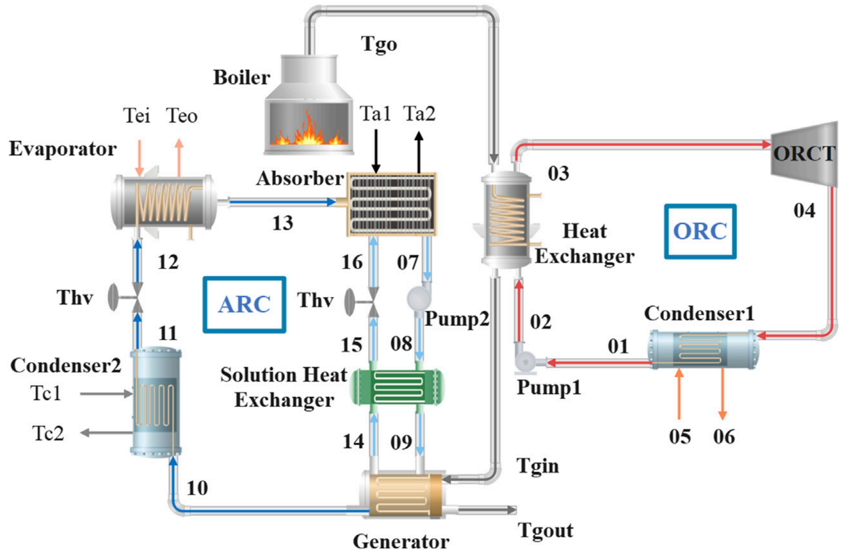

FIGURE 2
The flowchart of the proposed system.

working fluid is pressurized by pump 1 to the heat exchanger (02–03) and absorbs heat from the energy source fed to the heat exchanger, which is heated to high-temperature high-pressure vapor, which enters the Turbine to expand and generate electricity (03–04). Afterwards, it flows into the condenser 1 (04-01) and is condensed into a liquid by the refrigeration water, which then circulates through the ORC system again by pump 1 (01–02). In the absorption refrigeration cycle, water is the absorbent and ammonia is the refrigerant. We utilize waste heat from the heat exchanger to drive the heat source for the ARC system into the generator, where a concentrated solution of ammonia-water mixture is heated to evaporation, leaving a high temperature dilute solution. The high-pressure vapor is then condensed into a low temperature saturated liquid as it passes through condenser 2 (10–11), which is depressurized by the throttle valve and proceeds to the evaporator, which provides cooling through evaporation (11–13). The low-pressure ammonia steam is fed to the absorber (13-07) where it is diluted and absorbed into a concentrated solution into a concentrated solution of ammonia saturated water, which is sent under pressure to SHE via pump 2 to reclaim the waste heat of the concentrated solution in the generator (07–08). The dilute ammonia-water mixture remaining in the generator after the ammonia evaporation passes through SHE and returns to the absorber through a reduced pressure throttle valve (15–16).

3 Mathematical model

3.1 Thermodynamic model

The simulations of the waste heat recovery system in this study were implemented in MATLAB and all reactions were in thermodynamic equilibrium. The thermodynamic properties of the flue gas were calculated by REFPROP9.1 based on its basic composition: 58.14% N_2, 10.42% H_2O, 26.27% CO_2 and 5.17% O_2. The added system is composed of ORC and absorption refrigeration cycles, respectively, and the two subsystems are thermodynamically balanced for the new system by mass flow equilibrium on the generator and heat exchanger. Table 1 summarizes all the key input data of the system. In order to improve the effect of the system in practical application, the system parameters are rationalized. In order to ensure that the turbine can reach the target state in practical applications, the turbine efficiency is set to 70%, while the actual value is around 80% (Cai et al., 2016; Pethurajan et al., 2018). Men et al. (2021) compared the performance of different heat exchangers in practical applications, and the results showed the EW heat exchange efficiency was higher than 85%. In the theoretical design of this paper, the efficiency of the heat exchanger is set at 70%, lower than the actual value.

In the sub-section, a mathematical model based on thermodynamics as well as economics is established for the system. In order to streamline the model, some essential assumptions are defined:

(1) The subsystems operate at a steady state.
(2) The pumps and turbines operate at a specific isentropic efficiency.
(3) The pressure drop of piping is negligible.
(4) The low-temperature waste heat comes from the sugar mill exhaust gas at a temperature of about 190°C (Dogbe et al., 2018).
(5) The generator outlet refrigerant in ARC is superheated.

3.2 Energy analysis

On the basis of the mass balance equation (Eq. 1) and energy balance equation (Eq. 2) (Nami et al., 2019), the thermodynamic model of all parts of the subsystem was studied and the corresponding mass and energy equations were listed to easily analyze the system later, as shown in Table 2.

TABLE 1 Basic input parameters for ORC and ARC systems.

Parameter	Value
Ambient temperature, T_0 (K)	298.15
Ambient Pressure, P_0 (MPa)	0.101
Turbine efficiency, η_{ORCT} (%)	70 (Vaja and Gambarotta, 2010)
The isentropic efficiency of pump1, η_{P1} (%)	80 (Vaja and Gambarotta, 2010)
The isentropic efficiency of pump2, η_{P2} (%)	85 (Zare, 2020)
The isentropic efficiency of SHE, η_{SHE} (%)	80 (Zare, 2020)
Exhaust gas temperature, T_{go} (K)	463.15
Temperature difference of Cond1/Cond2 (K)	5 (Lu et al., 2020)
Temperature difference of HE (K)	30 (Lu et al., 2020)
The supply/return temperature of Eva, T_{ei}/T_{eo} (K)	280.15/285.15 (Lu et al., 2020)
The condense temperature of condenser 1, T_{Cond1} (K)	308
The condense temperature of condenser 2, T_{Cond2} (K)	303.15
Evaporation temperature of Eva, T_{Eva} (K)	278.15
Generation temperature of Gen, T_{Gen} (K)	353.15

TABLE 2 Control equations for each component of ORC and ARC.

Component	Energy balance equation
Heat Exchanger	$\dot{m}_g(h_{go}-h_{gin})=\dot{m}_2(h_3-h_2)$
ORCT	$\dot{W}_{ORCT}=\dot{m}_3(h_3-h_4), \dot{I}_{ORCT}=(h_3-h_4)/(h_3-h_{4s})$
Condenser1	$\dot{m}_4(h_4-h_1)=\dot{m}_5(h_5-h_6)$
Pump1	$\dot{W}_{P1}=\dot{m}_1(h_2-h_1), \dot{I}_{P1}=(h_{2s}-h_1)/(h_2-h_1)$
Generator	$\dot{m}_{13}h_{13}+\dot{m}_g h_{gin}=\dot{m}_7h_7+\dot{m}_{14}h_{14}+\dot{m}_g h_{gout}$
Condenser2	$\dot{m}_7(h_7-h_8)=\dot{m}_{c1}(h_{c1}-h_{c2})$
Evaporator	$\dot{m}_e(h_{ei}-h_{eo})=\dot{m}_9(h_{10}-h_9)$
Absorber	$\dot{m}_{16}h_{16}+\dot{m}_{a1}h_{a1}+\dot{m}_{20}h_{20}=\dot{m}_{11}h_{11}+\dot{m}_{a1}h_{a2}$
Solution Heat Exchanger	$\dot{m}_{12}(h_{13}-h_{12})=\dot{m}_{14}(h_{14}-h_{15}), \dot{I}_{SHE}=(T_{14}-T_{15})/(T_{14}-T_{12})$
Thv	$\dot{H}_8=\dot{H}_9, \dot{H}_{15}=\dot{H}_{16}$
Pump2	$\dot{W}_{P2}=\dot{m}_{11}(h_{12}-h_{11}), \dot{I}_{P2}=(h_{12s}-h_{11})/(h_{12}-h_{11})$

$$\sum \dot{m}_{in,k} = \sum \dot{m}_{out,k} \tag{1}$$

$$\dot{Q}_k + \sum \dot{m}_{in,k}h_{in,k} - \dot{W}_k - \sum \dot{m}_{out,k}h_{out,k} = 0 \tag{2}$$

Where *out* and *in* represent the outlet and inlet of the component, respectively. $\dot{W}$ as well as $\dot{Q}$ denote the power and heat transfer rate, respectively.

3.3 Exergy analysis

Exergy analysis has been widely used in the economic analysis of thermal systems that reveals the location, as well as the extent of process inefficiencies to optimize their capabilities and complements traditional mass flow analysis (Ghannadzadeh and Sadeqzadeh, 2017). The thermodynamic model of each component can be identified from the energy balance equation.

The exergy balance equation for the individual component is represented as Eq. 3 (Pan et al., 2021b):

$$\dot{E}_{Q,k} + \sum \dot{E}_{in,k} = \dot{E}_{w,k} + \sum \dot{E}_{out,k} + \dot{E}_{D,k} \tag{3}$$

The exergy value for each point is determined as Eq. 4 (Ebrahimi-Moghadam et al., 2021):

$$\dot{E}_{in} = \dot{m}\left[h_{in} - h_0 - T_0\left(s_{in} - s_0\right)\right] \tag{4}$$

TABLE 3 Exergy equations for each component of the system.

Component	$\dot{E}_f$	$\dot{E}_p$	$\dot{E}_D$
Heat Exchanger	$\dot{E}_{go} - \dot{E}_{gin}$	$\dot{E}_3 - \dot{E}_2$	$\dot{E}_{go} + \dot{E}_2 - \dot{E}_{gin} - \dot{E}_3$
ORCT	$\dot{E}_3 - \dot{E}_4$	$\dot{W}_{ORCT}$	$\dot{E}_3 - \dot{E}_4 - \dot{W}_{ORCT}$
Condenser1	$\dot{E}_4 - \dot{E}_1$	$\dot{E}_6 - \dot{E}_5$	$\dot{E}_4 + \dot{E}_5 - \dot{E}_1 - \dot{E}_6$
Pump1	$\dot{W}_{P1}$	$\dot{E}_2 - \dot{E}_1$	$\dot{W}_{P1} + \dot{E}_1 - \dot{E}_2$
Generator	$\dot{E}_{gin} - \dot{E}_{gout}$	$\dot{E}_{14} + \dot{E}_7 - \dot{E}_{13}$	$\dot{E}_{gin} + \dot{E}_{13} - \dot{E}_{gout} - \dot{E}_{14} - \dot{E}_7$
Condenser2	$\dot{E}_7 - \dot{E}_8$	$\dot{E}_{c2} - \dot{E}_{c1}$	$\dot{E}_7 + \dot{E}_{c1} - \dot{E}_8 - \dot{E}_{c2}$
Evaporator	$\dot{E}_{10} - \dot{E}_9$	$\dot{E}_{ei} - \dot{E}_{eo}$	$\dot{E}_{10} + \dot{E}_{eo} - \dot{E}_9 - \dot{E}_{ei}$
Absorber	$\dot{E}_{10} + \dot{E}_{16} - \dot{E}_{11}$	$\dot{E}_{a2} - \dot{E}_{a1}$	$\dot{E}_{10} + \dot{E}_{16} + \dot{E}_{a1} - \dot{E}_{11} - \dot{E}_{a2}$
Solution Heat Exchanger	$\dot{E}_{14} - \dot{E}_{15}$	$\dot{E}_{13} - \dot{E}_{12}$	$\dot{E}_{14} + \dot{E}_{12} - \dot{E}_{15} - \dot{E}_{13}$
Pump2	$\dot{W}_{P2}$	$\dot{E}_{12} - \dot{E}_{11}$	$\dot{W}_{P2} + \dot{E}_{11} - \dot{E}_{12}$

The detailed exergy equations for each component are concluded in Table 3.

3.4 Economic analysis

Integrated sugar mill flue gas waste heat recovery system should consider not only thermodynamic aspects but also matters such as economic costs. The Levelized Cost Of Energy (*LCOE*) is one of the more extensively employed criteria in the feasibility analysis of evaluating new generation systems and power plants (Boukelia et al., 2016). The relationship between *LCOE* and annual system power generation and input costs is calculated using Eq. 5:

$$\boldsymbol{LCOE = CRF \times Z_{investment} + Z_{OM} / 8760 \times (W_{\mathrm{net}} + E_{cool})} \tag{5}$$

Where $Z_{investment}$ is the overall investment cost of the system ($), Z_{OM} is the operation and maintenance cost ($). To estimate the annual operation as well as maintenance cost, the maintenance factor was chosen as 0.04 (Bhattacharyya and Quoc Thang, 2004).

CRF indicates the capital recovery factor calculated by Eq. 6:

$$\boldsymbol{CRF = i(1+i)^n / (1+i)^n - 1} \tag{6}$$

Where i and n are the interest rate ($i = 0.1$) as well as the lifetime of the system (n = 20 years) (Zhang et al., 2018), respectively. $Z_{investment}$ is composed of the investment cost data for the whole system components. Some cost equations from references (Khaljani et al., 2015; Lu et al., 2020; Nami and Anvari-Moghaddam, 2020; Pan et al., 2021a; Pan et al., 2021b) are applied to the main equipment of this system: turbine, pump and Generator, etc. The investment cost of each component can be calculated by the cost function given in Table 4. It is worth mentioning that the value of the valves is small compared to the other components, so their investment cost is ignored for procurement.

Considering the Chemical Engineering Plant Cost Index (CEPCI) of 699.97 in 2021 (The Chemical Engineering Plant Cost Index, n.d.), the cost function in Table 4 was updated to the year 2021 according to Eq. 7.

TABLE 4 The cost functions of each component.

Component	Cost function	Year
Heat Exchanger	$Z = 309.14 A_{HE}^{0.85}$	2001
ORCT	$Z = 6000 \dot{W}_{ORCT}^{0.7}$	2013
Condenser1	$Z = 280.74 \times \dot{Q}_{cond2}/2.2\Delta T_{cond1} + 746\dot{m}_5$	2018
Pump1	$Z = 3540 \dot{W}_{P1}^{0.71}$	2011
Generator	$Z = 17500\,(A_{Gen}/100)^{0.6}$	2015
Condenser2	$Z = 280.74 \times \dot{Q}_{cond2}/2.2\Delta T_{cond2} + 746\dot{m}_{c1}$	2018
Evaporator	$Z = 16000\,(A_{Eva}/100)^{0.6}$	2000
Absorber	$Z = 16000\,(A_{Abs}/100)^{0.6}$	2000
Solution Heat Exchanger	$Z = 309.14 A_{SHE}^{0.85}$	2001

$$\boldsymbol{\dot{Z}_{k,2021} = \dot{Z}_k \times CEPCI_{2021} / CEPCI_{ref}} \tag{7}$$

Based on the total investment cost and annual net income, the system's investment payback cycle PP can be estimated as Eq. 8 (Wang et al., 2015):

$$\boldsymbol{PP = \frac{Z_{tot}}{NE}} \tag{8}$$

Where Z_{tot} is the total cost, NE is the annual net income.

Z_{tot} is composed of equipment investment cost (Z_B) and maintenance cost (Z_{OM}), which is calculated using Eq. 9:

$$\boldsymbol{Z_{tot} = Z_B + Z_{OM}} \tag{9}$$

The annual net income (NE) is determined by the net output power, electricity price, refrigeration capacity, and cooling water price, which is calculated using Eq. 10:

$$\boldsymbol{NE = p_e (W_{ORCT} - W_{p1}) \times 8760 + E_{cool} \times p_{cw} \times 8760} \tag{10}$$

Where p_e is the price of electricity, with a value of 0.11 $/kWh, p_{cw} is the price of cooling water, with a value of 0.35 $/GJ (Liu et al., 2020).

TABLE 5 Total heat transfer coefficient of each component.

Component	U (kW/m²·K)
Heat Exchanger	0.8786
Absorber	0.8
Generator	1.3
Evaporator	1.1
Solution Heat Exchanger	0.7

For the heat transfer area of each component, the calculation is performed by Eq. 11 (Li et al., 2019):

$$A_k = \dot{Q}_k / (U_k \times \Delta T_{k,LMTD}) \tag{11}$$

$\dot{Q}_k$ is the heat transfer rate of each component, and U_k is given specifically in Table 5. ΔT_{LMTD} is the logarithmic mean temperature difference (Eq. 12):

$$\Delta T_{k,LMTD} = (\Delta T_{k,A} - \Delta T_{k,B}) / \ln(\Delta T_{k,A} / \Delta T_{k,B}) \tag{12}$$

Where $\Delta T_{k,A}$ and $\Delta T_{k,B}$ represent the temperature difference between the cooling and heating streams for each component, respectively.

3.5 Performance evaluation

To evaluate the capacity of the waste heat recovery system, some concepts is calcluated using Eqs 13–15:

$$\dot{W}_{net} = \dot{W}_{ORCT} - \dot{W}_{P1} - \dot{W}_{P2} \tag{13}$$

$$\dot{Q}_e = \dot{m}_e (h_{ei} - h_{eo}) \tag{14}$$

$$\dot{Q}_g = \dot{m}_g (h_{go} - h_{gin}) \tag{15}$$

$\dot{W}_{net}$ and $\dot{Q}_e$ represent the net power output of the whole system and the heat transfer rate of the evaporator, respectively. $\dot{W}_{ORCT}$ is the net power output of the turbine, $\dot{W}_{P1}$ and $\dot{W}_{P2}$ are the power consumption of pump1 and pump2, respectively. $\dot{Q}_g$ is the heat transfer rate delivered to the ARC.

The cooling exergy of the system is defined as Eq. 16:

$$\dot{E}_{cool} = \dot{E}_{eo} - \dot{E}_{ei} \tag{16}$$

The equation for the thermal efficiency of the systemis defined as Eq. 17:

$$COP = \frac{\dot{Q}_e}{\dot{Q}_g} \tag{17}$$

The exergy efficiency formula for the system is defined as Eq. 18:

$$\eta_{Ex} = (\dot{W}_{net} + \dot{E}_{cool}) / (\dot{E}_{go} - \dot{E}_{gout}) \tag{18}$$

$\dot{E}_{go}$ is the input exergy of the system, which is the boiler flue gas exergy for the sugar mill. $\dot{E}_{gout}$ is the output exergy of the whole system.

3.6 Multi-objective optimization

To resolve the conflict between economic factors and the thermodynamic performance of the cycle, a non-dominated ranking genetic algorithm II (NSGA-II) is adopted for the multi-objective optimization of the cascaded system (Tan et al., 2023). As in Figure 3, the objective function, decision variables and constraints are the three elements of the optimization problem, and η_{Ex} and $LCOE$ are taken as the objectives to achieve the lowest cost optimum exergy efficiency η_{Ex} and to obtain the appropriate system operating conditions. The decision-making variables and the range of values are shown in Table 6. The parameters of the genetic algorithm are summarized in Table 7. The flow chart of NSGA-II is shown in Figure 4.

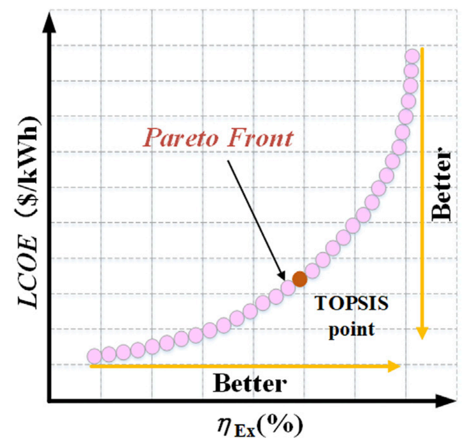

FIGURE 3
Graphical representation of the Pareto front of an objective optimization problem.

TABLE 6 Decision variables and their ranges.

Decision variables	Range of variables
Heat exchanger pressure, P_{orc_eva} (kPa)	900–2,200
Evaporator temperature, T_{eva} (K)	274.15–279.15
Generator temperature, T_{gen} (K)	349.15–355.15

3.7 Validation

To confirm the accuracy of the system model, the key subsystems of the built system were verified. The key subsystems include the ORC and the absorption refrigeration cycle, and the modeling of each subsystem were validated individually using experimental data from the literature. To validate the ORC model, results from the literature (Vaja and Gambarotta, 2010) were used for comparison. The ARC model was also validated using the literature (Zare, 2020). As shown in Tables 8, 9, there is excellent concordance between the findings of the current study and the data presented in the literature (Vaja and Gambarotta, 2010; Zare, 2020). Therefore, the accuracy of the current study results was verified. As can be seen from Figure 5, the simulation results of this study are in excellent consistency with references.

TABLE 7 Adjustable parameters used for the optimization.

Parameters	Value
Population size	15
Number of maximum generation	100
Probability of crossover	90%
Probability of mutation	10%
Selection process	Tournament
Tournament size	2

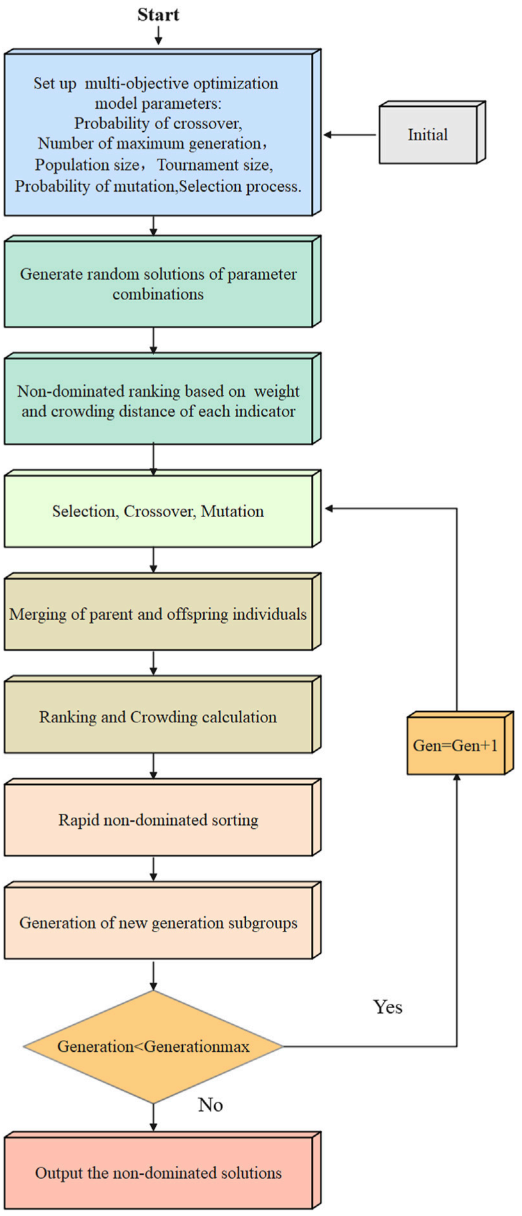

FIGURE 4
The flow chart of NSGA-II.

4 Results and discussion

This section discusses and analyzes a new system developed based on waste flue gas from sugar mills after bagasse combustion with ORC and absorption refrigeration system composition. The analysis is carried out for parameters such as evaporation temperature and generator temperature to summarize the conclusions. Bagasse is composed of 0.8% wax, 2.3% ash, 18.1% lignin, 33.8% hemicellulose, as well as 43.6% cellulose (Nemomsa et al., 2022). Bagasse is burned in the sugar mill to provide steam for the sugar mill process, however a significant quantity of low-temperature heat is still emitted to the atmosphere with the flue gas. The heat source in the ORC system is the flue gas from the sugar mill (190°C) (Dogbe et al., 2018), and has a high exergy content of 11.95 MW. This paper presents the system's exergy, mass flow rate, distribution of fire loss of each component, and multi-objective optimization results.

4.1 The analysis of ORC working fluid

The operational performance of waste heat recovery systems is affected by the properties of the organic working fluid. Examples of ideal working fluid properties include suitable boiling point temperature, lower latent heat, higher critical temperature and pressure, appropriate specific volume, higher thermal conductivity, lower density and surface tension, non-corrosive, higher thermal stability, non-toxic, zero ODP, as well as low GWP (Hung et al., 1997; Luo et al., 2015). In addition, the closer the critical temperature of the working fluid is to the temperature of the heat source, the higher the performance of the system will be (Lu et al., 2020). Based on the aforementioned conditions, nine organic working fluids were screened, as shown in Table 10. By comparing the operation results under the same working conditions, the ORC working fluids with more ideal conditions were obtained.

The net power output of ORC is reflective of the performance of the waste heat recovery system. Therefore, in the present research, the net power output was determined as the target value, and the net power output ($\dot{W}_{orc\_net}$) was tested by varying the evaporator temperature of the ORC system (P_{orc_eva}). The net power output of the ORC system ($\dot{W}_{orc\_net}$) at nine organic working fluids was analyzed by setting the evaporator pressure in the organic Rankine cycle from 900 to 2,200 kPa. As shown in Figure 6, Pentane, Isopentane and R245ca can reach the highest point of $\dot{W}_{orc\_net}$ at the lowest pressure operating conditions, for example, when the working fluid is Pentane, P_{orc_eva} = 900 kPa, $\dot{W}_{orc\_net}$ = 569.43 kW, as the evaporator pressure continues to increase, the performance of the three working fluids gradually decreases, indicating that the working fluids are not suitable for operation in this pressure region. The six organic working fluids except for Pentane, Isopentane and R245ca gradually increase with increasing evaporator pressure in the constrained region, and the net power gradually moves toward the highest point. The increase in evaporator pressure P_{orc_eva}, although it raises $\dot{W}_{orc\_net}$, also puts an additional burden on the system, which in return causes to an increase in cost, so a suitable value

TABLE 8 The results of comparison between present work and Ref. (Vaja and Gambarotta, 2010).

	Present work	References (Vaja and Gambarotta, 2010)	Error (%)
Evaporation temperature of Eva (K)	494.58	494.4	−0.04
Evaporation pressure of Eva (kPa)	2000	2000	0
The condense pressure of Condenser (kPa)	19.66	19.6	−0.30
$\triangle h_{3'-4}$ (kJ/kg)	130.5	130.5	0
Efficiency of ORC (−)	0.1978	0.1986	0.40
Power of ORC (kW)	348.52	349.3	0.22
V_4/V_3 (−)	107.78	107	−0.73

TABLE 9 The results of comparison between present work and Ref. (Zare, 2020).

Points	P (kPa)			T (K)		
	This work	Ref. (Zare, 2020)	Error (%)	This work	Ref. (Zare, 2020)	Error (%)
17	11.7	11.7	0	353.2	353.2	0
18	11.7	11.7	0	303.2	303.2	0
19	4.3	4.3	0	273.2	273.2	0
20	4.3	4.3	0	273.2	273.2	0
21	4.3	4.3	0	301.9493	303.2	0.4142
22	11.7	11.7	0	302.0561	303.2	0.3787
23	11.7	11.7	0	334.8610	336.4	0.4596
24	11.7	11.7	0	351.5131	353.2	0.4799
25	11.7	11.7	0	311.9474	313.2	0.4015
26	4.3	4.3	0	315.4779	313.4	0.6587

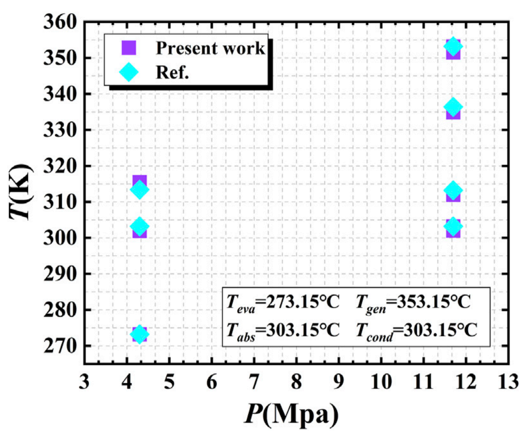

FIGURE 5
Model authentication between present study with Ref.

needs to be found between evaporator pressure and $\dot{W}_{orc\_net}$. When considering the specific application of the working fluid, attention needs to be paid to its latent heat properties Pentane, Isopentane and R245ca have the highest net power upfront in the ORC system, but as P_{orc_eva} increases, their latent heat decreases more rapidly than other working fluids, leading to a more rapid reduction in system efficiency and a decrease in heat transfer between the flue gas as well as the organic working fluid. Both Butane and R245fa have relatively close critical temperatures, but Butane has a slightly lower critical temperature, which is closer to the waste heat temperature. Additionally, Butane has a lower triple point temperature, which may contribute to better liquefaction performance. Selecting Butane as the working fluid in the ORC can reduce energy waste within the system and provide additional thermal energy for the ARC, potentially offering enhanced refrigeration effects. Furthermore, Butane exhibits better energy efficiency and has a lesser impact on the environment due to its lower ozone depletion potential (ODP) and global warming potential (GWP).

4.2 Parametric study

4.2.1 High pressure in ORC analysis

The outlet pressure of Pump1, as the highest pressure in the ORC system, affects many factors in the system, for example, the heat load of the heat exchanger. Therefore, it is an important

TABLE 10 The thermodynamic properties of selected organic fluids.

Working fluid	Temperature limit T_L (K)	Critical point		Triple point T_T (K)	Normal boiling T_B (K)
		T_C(K)	P_C(MPa)		
R245fa	171.05 to 440.0	427.16	3.651	171.05	288.29
R245ca	191.5 to 450.0	447.57	3.9407	191.5	298.41
R236fa	179.6 to 400.0	398.07	3.2	179.6	271.66
Isobutane	113.73 to 575.0	407.81	3.629	113.73	261.4
Butane	134.9 to 575.0	425.13	3.796	134.9	272.66
Isopentane	112.65 to 500.0	460.35	3.378	112.65	300.98
Pentane	143.47 to 600.0	469.7	3.37	143.47	309.21
R1234ze	168.62 to 420.0	382.51	3.6349	168.62	254.18
R236ea	240.0 to 412.0	412.44	3.42	170.0	279.32

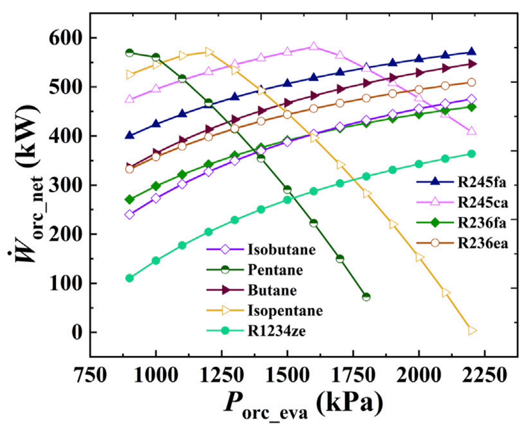

FIGURE 6
Net output power of ORC system by different organic working substances.

object of study in this research. As shown in Figures 7A–F, this study analyzes the effect of Pump1 outlet pressure on $\dot{W}_{net}$ for different T_{ARC_Eva} operating conditions. For the same Pump1 outlet pressure, the higher the evaporator temperature, the greater the variation in the values of $\dot{W}_{net}$ and η_{Ex}, For example, when the working fluid is R236ea and Pump1 outlet pressure = 1,400 kPa, $\dot{W}_{net}$ = 419.62 KW (T_{ARC_Eva} = 1°C), $\dot{W}_{net}$ = 420.15 KW (T_{ARC_Eva} = 3°C), $\dot{W}_{net}$ = 420.65 KW (T_{ARC_Eva} = 5°C). After Pentane, Isopentane and R245ca reached the peak early relative to the other six working fluids, the increasing trend gradually disappeared with the increase of pressure. The remaining six organic working fluids show a slowly increasing trend in general. If the isentropic efficiency of the turbine is kept constant, $\dot{W}_{net}$ can be increased by increasing the maximum pressure, but with the pressurization of Pump1, it is difficult to sustain the consistency of turbine efficiency, which eventually leads to increased destruction in other components.

As shown in Figure 7F, when Pump1 outlet pressure = 2,100 kPa and other working conditions are the same, the total exergy system efficiency η_{Ex} from largest to smallest is R245fa, Butane, R236ea, R245ca, Isobutane, R236fa, R1234ze, Isopentane, and Pentane, moreover, the $\dot{W}_{net}$ and η_{Ex} of Butane showed an increasing trend with continuous pressurization, verifying the choice of Butane as the best working fluid.

4.2.2 The effect of evaporator temperature

Based on the comprehensive research on the performance impact of various organic working fluids on the ORC system, it was found that Butane provides superior benefits compared to other fluids. Therefore, in the subsequent analysis, we have chosen Butane as the working fluid for the ORC system. The evaporator temperature in the absorption refrigeration cycle is a key design parameter, and Figure 8 presents the impact of evaporator temperature on the exergy efficiency (η_{Ex}) and the net system output power ($\dot{W}_{net}$) under the condition where the heat source temperature is set at 190°C and the ORC working fluid is Butane. It is evident that $\dot{W}_{net}$ and η_{Ex} improves with the increase of evaporator temperature. When the temperature of the evaporator falls within the range of 274.15°C–279.15°C, enhancing the evaporator temperature enhances the efficacy of the waste heat recovery system. This is because of the simultaneous rise in both evaporator pressure and temperature, resulting in a substantial augmentation in the absorption efficiency of the diluted solution, leading to a noteworthy enhancement in effectiveness.

4.2.3 The effect of generator temperature

The temperature of the generator is also an important parameter to study when designing the ARC system, heat transfer rate of condenser2 ($\dot{Q}_{cond2}$), and the total net output of the system $\dot{W}_{net}$ as well as the exergy efficiency η_{Ex} are plotted in Figure 9. The graph shows that the generator temperature changes from 349.15 K to 355.15 K, as the generator temperature increases, the exergy efficiency of the system η_{Ex} gradually improves, while the net output power varies in the opposite trend. The reason is that as the temperature of the generator continues to rise, the solubility of the absorber is greater, the amount of solution circulation is reduced, the power consumption of the pump is

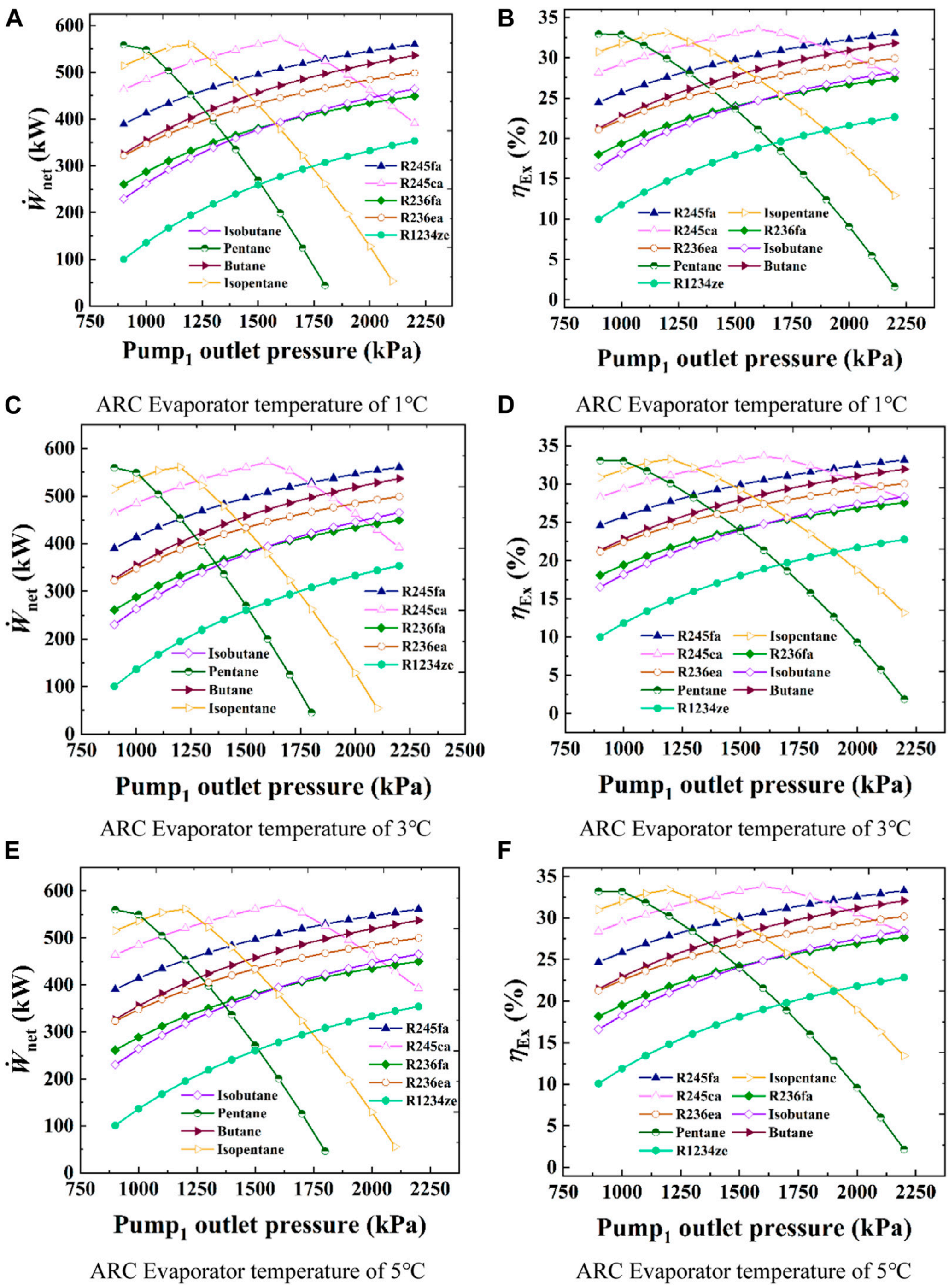

FIGURE 7
Effect of high pressure in ORC on $\dot{W}_{net}$. **(A)** ARC Evaporator temperature of 1°C. **(B)** ARC Evaporator temperature of 1°C. **(C)** ARC Evaporator temperature of 3°C. **(D)** ARC Evaporator temperature of 3°C. **(E)** ARC Evaporator temperature of 5°C. **(F)** ARC Evaporator temperature of 5°C.

lessened, and the evaporator absorbs more heat, resulting in a reduction in the thermal load of the component, ultimately increasing η_{Ex} and reducing the net output power. For example, as shown in Figure 9, the variation trend of the heat transfer rate of the condenser is listed. As the temperature of the generator rises, $\dot{Q}_{cond2}$ gradually decreases, so the η_{Ex} increases and the $\dot{W}_{net}$ decreases.

4.2.4 The effect of ORC evaporator pressure and condenser temperature

In an organic Rankine cycle (ORC) system, the maximum working pressure (P_{max}) and condenser temperature (T_{cond1}) have a significant impact on several performance parameters of the whole system, as depicted in Figures 10A–D. The results indicate that increasing the maximum working pressure of the ORC system

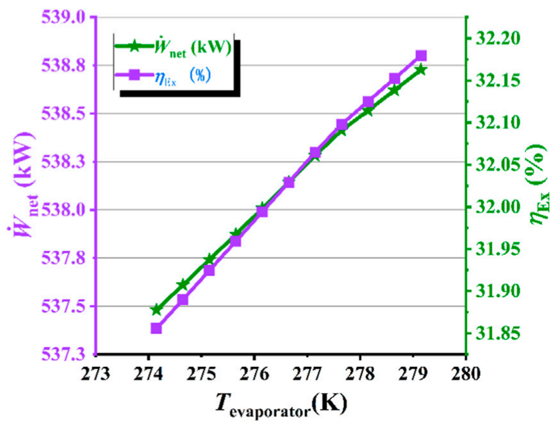

FIGURE 8
Effect of ARC evaporator temperature on the net system output power $\dot{W}_{net}$ and the exergy efficiency η_{Ex}.

can markedly enhance the net power output and exergy efficiency (η_{Ex}) of the system. When maintaining a constant condenser temperature, elevating the maximum pressure results in an increase in turbine efficiency, with the net turbine power growing at a rate faster than the energy consumption of the pumps, thereby augmenting the net output power of the system. This series of enhancements will exert a positive influence on the input costs and *LCOE* of the system, thereby enhancing the system's economic viability. The input cost experiences a significant decrease when T_{cond1} exceeds 304 K. The primary reason for this phenomenon is that the temperature of the T_{cond1} leads to a greater temperature differential for the working fluid in ORC during the expansion process, consequently enhancing power generation performance. Furthermore, the higher condenser temperature signifies a reduction in the surface area of the heat exchanger, reducing the size and cost of the heat exchanger within the system, subsequently lowering the energy recovery costs, resulting in a reduction in the *LCOE*.

4.2.5 The effect of ARC evaporator temperature and condenser temperature

The effects of ARC evaporator temperature and condenser temperature on the net output power, exergy efficiency, total investment, and *LCOE* of the system are shown in Figures 11A–D. The results indicate that decreasing the condenser temperature (T_{cond2}) and increasing the evaporator temperature ($T_{evaporator}$) in the ARC system enhance the net power output and exergy efficiency. As the ARC condenser temperature rises, the entry temperature of the working fluid must also increase to match the heat source, leading to increased operating costs for the system. Although investment generally shows a downward trend, the additional cost of increasing the temperature outweighs the benefits of heat recovery, resulting in an increase in *LCOE*. To ensure optimal system performance and economics, it is crucial to have an economically viable energy recovery solution available for the system and select the appropriate turning point of the *LCOE* versus input cost surface, for example, T_{cond2} = 303.15.

4.2.6 The effect of generator temperature and condenser temperature

Figures 12A–D illustrates the impact of ARC generator temperature and condenser temperature on the net output power, exergy efficiency, total investment, and *LCOE* of the overall system. While keeping T_{cond2} constant, the system's exergy efficiency improves with an increase in generator temperature. As depicted in Figs. c–d, the rise in generator temperature necessitates the use of costlier materials to withstand the high-temperature environment, leading to a concomitant increase in both total investment and *LCOE*.

4.3 The analysis of exergy destruction in the component

Figure 13 presents the findings of the exergy analysis based on the design conditions for the waste heat recovery system. The primary function of Pump2 is to enhance heat transfer efficiency, rather than being the primary workload in the circulation system,

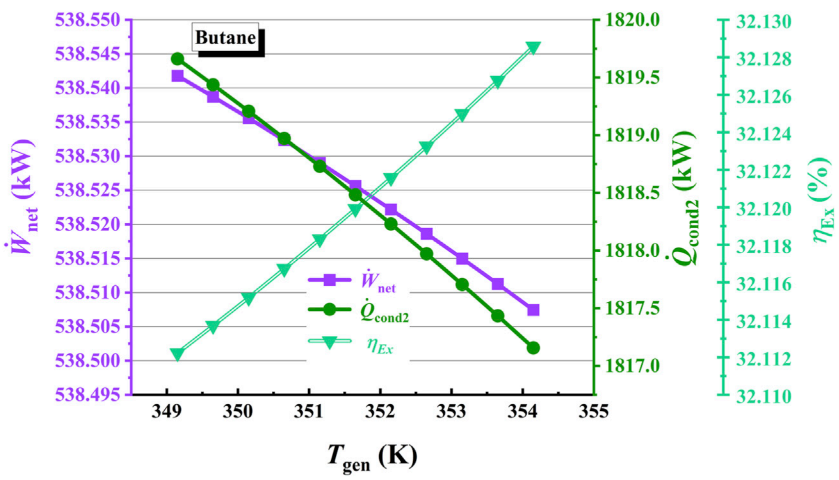

FIGURE 9
Effects of generator temperature on $\dot{Q}_{cond2}$, $\dot{W}_{net}$ and η_{Ex}.

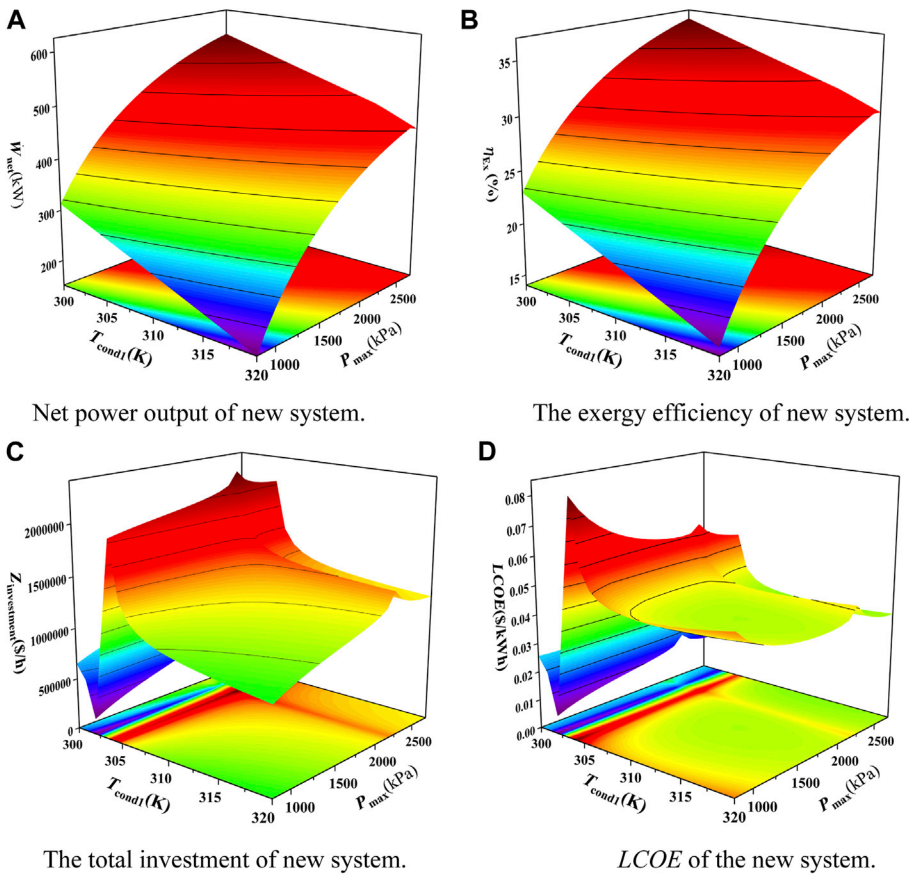

FIGURE 10
Effects of ORC evaporator pressure and condenser temperature on the system. **(A)** Net power output of new system. **(B)** The exergy efficiency of new system. **(C)** The total investment of new system. **(D)** *LCOE* of the new system.

hence the negligible impact of Pump2 can be neglected. 50.8% of exergy destruction in the system occurs in the generator, followed by the evaporator and absorber. This is because of the high-temperature ammonia mixture solution under isobaric conditions, which causes the generator to operate at elevated temperatures. As a result, it concentrated most exergy destruction in the generator and absorber. These irreversibilities are mainly due to mixing destruction in the generator and absorber as well as to concentration gradients, temperature gradients and external forces (Nami et al., 2017). The exergy destruction in the ORC system occurs mainly in the HE (6.79%), and the high value of energy destruction is primarily caused by the large temperature discrepancy that exists between the cold and hot flows in the component (Aman et al., 2014). This figure shows the need to consider the design of the generator, absorber and Heat Exchanger to reduce exergy destruction by them. The thermodynamic properties of the system are shown in Table 11.

4.4 The results of economic analysis

The economic efficiency is an effective factor to judge the sustainability of the system, which depends not only on the exergy efficiency of the system but also on the net output efficiency and the *LCOE*, as shown in Table 12 for the new sugar plant. The investment cost of the new system is 2.94 million dollars (M$). It can be concluded from Figure 14 that the overall cost of the ORC cycle is based higher than the cost of the ARC cycle. In addition, the ORC system has the highest heat exchanger cost. However, by recycling the system, the net power output is increased by 0.5385 MW, providing 4717.26 MW of renewable electricity and 15,820.56 MW of space cooling capacity for the sugar plant per year. The payback period of the system is 5.79 years. The economic performance of the system is highly dependent on the price of renewable electricity, and the higher the price, the more investment potential the project has. The results of the economic analysis of the system illustrate that the waste heat recovery system of the sugar mill has a great economic potential, and the project is economically feasible.

4.5 Multi-objective optimization results

In this study, we employ NSGA-II to identify optimal system operation parameters in order to address the trade-off between

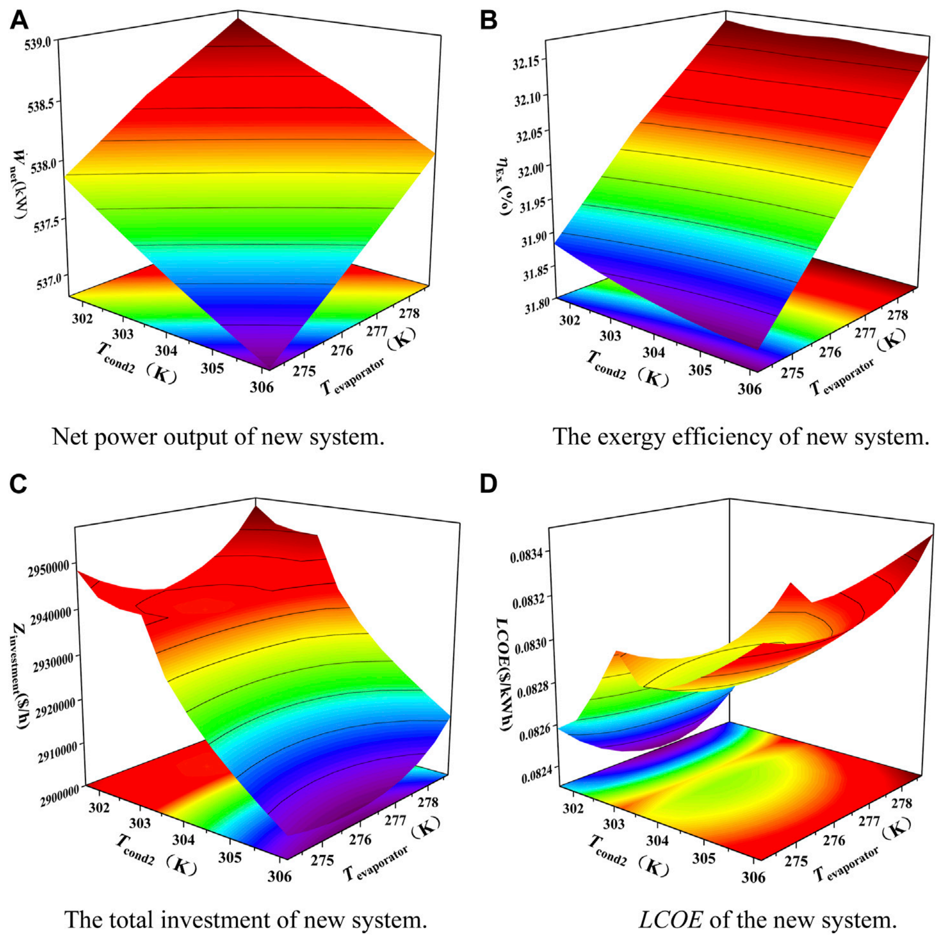

FIGURE 11
Effects of ARC evaporator pressure and condenser temperature on the system. **(A)** Net power output of new system. **(B)** The exergy efficiency of new system. **(C)** The total investment of new system. **(D)** *LCOE* of the new system.

LCOE and exergy efficiency η_{Ex} Figure 15 illustrates the Pareto front solutions for both the ORC and ARC systems. The Pareto Frontier represents potential executable plans at various points, typically selected based on the decision maker's objectives. Points A and B correspond to two optimal solutions, one with the minimum *LCOE* and the other with the maximum η_{Ex}, respectively. Point C represents an ideal scenario that satisfies both the minimum *LCOE* and the maximum η_{Ex}. However, due to the inherent conflict between these two objectives, they cannot be simultaneously achieved. Therefore, we employ the results of the TOPSIS analysis to identify point D, which is closest to point C and thus considered the best available solution. This solution represents the optimal system operation parameters, as detailed in Table 12. The results after running are shown in Table 13. The optimized η_{Ex} achieved a significant increase to 31.57%, demonstrating substantial improvement. Notably, in terms of economic indicators, the *LCOE* has effectively converged with the electricity price, reaching a reduced value of 0.0406$/kWh. This clearly indicates the waste heat recovery system's slight but discernible economic advantage. In order to comprehensively assess the economic returns of the entire system, the purchase prices for electricity and cooling have been set at an average annual rate of €30 per MWh and €20 per MWh (Nami and Anvari-Moghaddam, 2020). Furthermore, the implementation of the optimized system is expected to yield an annual revenue of $136,300 from electricity sales, while also resulting in substantial savings of around $308,600 in cooling expenses. When considering the overall outcomes, these optimization results establish a viable solution characterized by both remarkable economic efficiency and notable technical advantages.

4.6 Comparison of multiple systems and single system

Malwe et al. (2021) proposed a VCRS-ORC system aiming to achieve waste heat recovery, cooling, and electricity generation. The final exergy efficiency of this system was determined to be 17.95%, with a net output power of 0.296 kW. In this study, an ORC-ARC system was introduced to achieve higher energy utilization efficiency. Compared to the former, the exergy efficiency of this system increased by 14.175%, reaching a net output power of

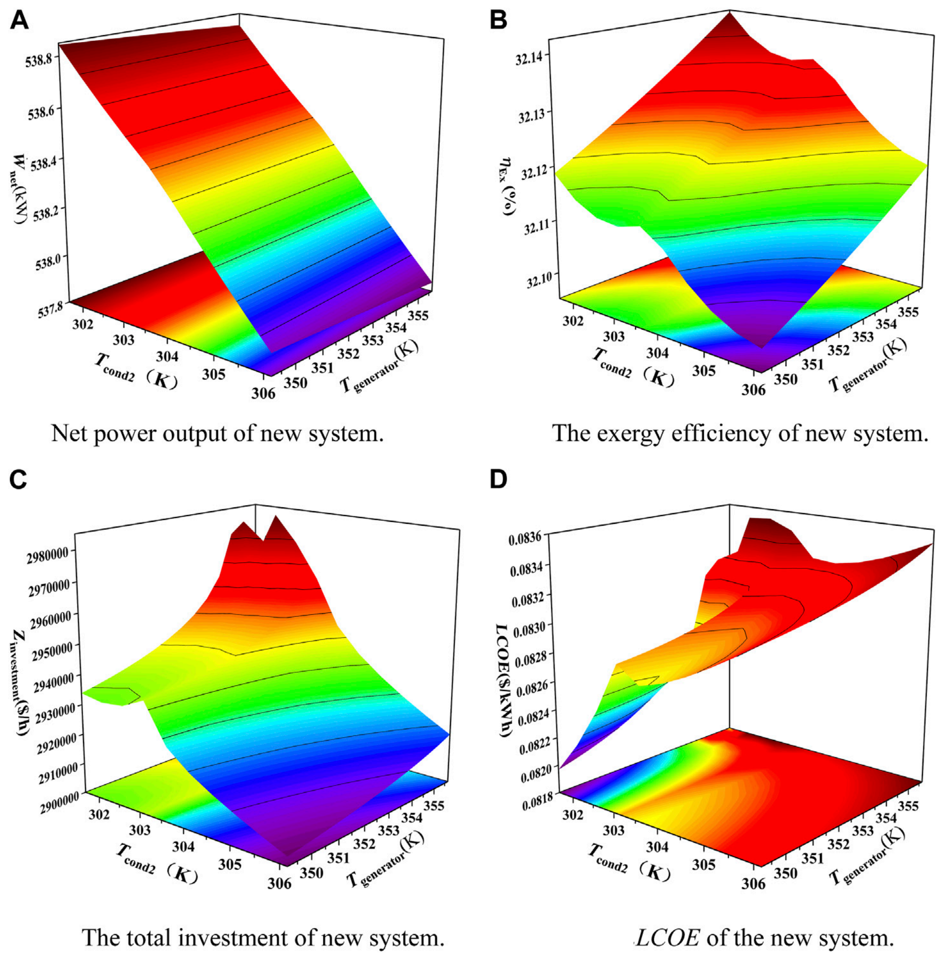

FIGURE 12
Effects of ARC Generator pressure and condenser temperature on the system. **(A)** Net power output of new system. **(B)** The exergy efficiency of new system. **(C)** The total investment of new system. **(D)** *LCOE* of the new system.

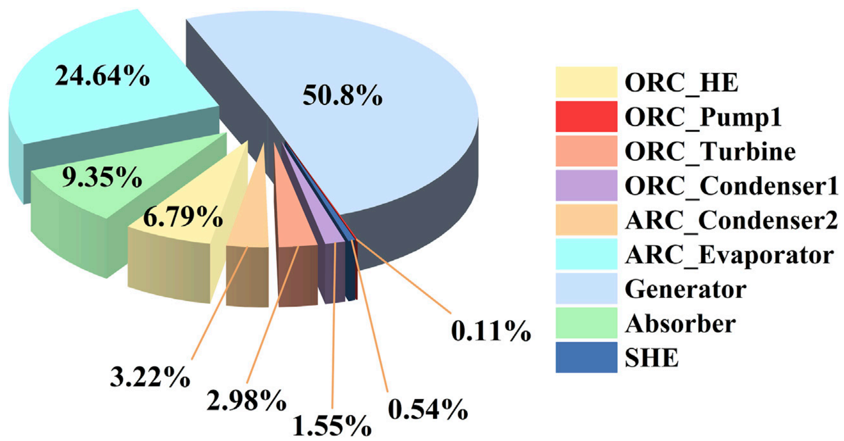

FIGURE 13
The exergy destruction rate of each component of the system.

TABLE 11 The parameters of each stream.

Stream	Fluid	T (K)	P (kPa)	m (kg/s)	h (kJ/kg)	s (kJ/(kg·K))
1	Butane	308.00	326.94	10.76	283.84	1.29
2	Butane	309.22	2213.11	10.76	288.03	1.29
3	Butane	393.15	2213.11	10.76	740.69	2.51
4	Butane	334.61	326.94	10.76	685.59	2.58
7	Ammonia	353.15	1167.20	1.61	1617.46	5.21
8	Ammonia	303.15	1167.20	1.61	484.91	1.96
9	Ammonia	278.15	515.75	1.61	484.91	6.03
10	Ammonia	278.15	515.75	1.61	1610.55	6.03
11	AWM X = 0.534	307.63	515.75	9.92	90.76	1.09
12	AWM X = 0.534	307.73	1167.20	9.92	91.72	1.09
13	AWM X = 0.534	336.55	1167.20	9.92	229.82	1.52
14	AWM X = 0.444	351.51	1167.20	8.31	263.75	1.58
15	AWM X = 0.444	316.48	1167.20	8.31	98.97	1.09
16	AWM X = 0.444	321.40	515.75	8.31	121.27	1.16
Tgo	flue gas	463.15	101.00	62.63	772.93	6.53
Tgin	flue gas	393.15	101.00	62.63	695.13	6.35
Tgout	flue gas	356.55	101.00	62.63	655.06	6.24

TABLE 12 The economic analysis of the new system.

	Value
Total investment cost (M$)	2.94
Net power output (MW)	0.5385
Net annual power supply (MW h)	4717.26
Annual cooling capacity provided (MW)	15,820.56
LCOE ($/kWh)	0.0830
Payback period (year)	5.79
Exergy efficiency (%)	32.125

5,385 kW. Significantly improved system efficiency and power output were achieved by studying the optimal working fluid in the ORC and analyzing key factors within the system.

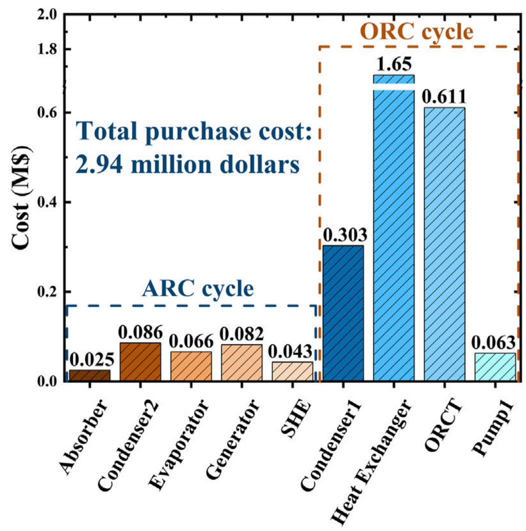

FIGURE 14
Cascade system component cost.

4.7 Possible differences in real exploitation conditions

First, in the actual operation process, the heat exchanger may not reach the ideal pinch point designed, resulting in a large temperature difference and failure to achieve the desired performance. Second, the efficiency of pumps and turbines depends on variable operating conditions. The optimal working conditions of the pump and the turbine may be difficult to achieve, resulting in reduced system performance. The characteristics of the heat source affect the performance of ORC. In the actual operation process, heat source fluctuations will reduce the efficiency of the steam turbine and the effectiveness of the heat exchanger, so the performance may be reduced.

TABLE 13 Pareto-optimal solutions for the system operation.

Parameter	Value
P_{ORC_Eva} (kPa)	2100.10
T_{ARC_Eva} (K)	277.2458
T_{Gen} (K)	349.6879
η_{Ex} (%)	31.57
LCOE ($/kWh)	0.040648

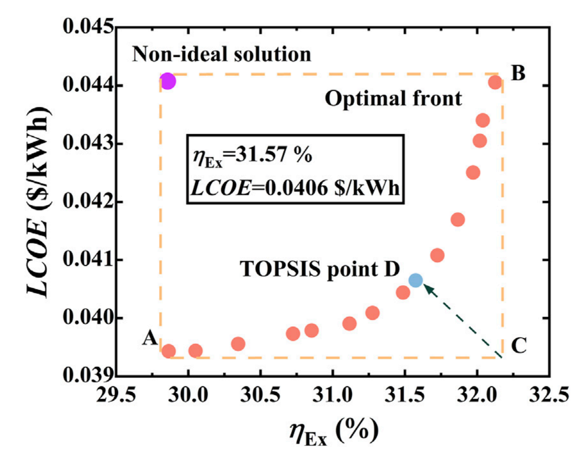

FIGURE 15
System Pareto front solution with *LCOE* and exergy efficiency η_{Ex} as the objective function.

5 Conclusion

This research presents a novel waste heat recovery system composed of an absorption refrigeration cycle and an organic Rankine cycle, which is applied for the recovery of boiler flue gas in a sugar factory. By taking the utilization of flue gas, considerable power generation and refrigeration output are obtained, resulting in improvements in system irreversibility and exhaust emissions. An economic and thermodynamic analysis of the entire system are conducted. The main conclusions are summarized as:

(1) In this research, nine working fluids were adopted and among which Butane was identified as the most appropriate working fluid for ORC.
(2) With an investment of 2.94 million dollars (M$), the system has a high exergy efficiency of 32.125%, with an increased power output of 4717.26 MW h and an increased space cooling capacity of 15,820.56 MW per year for the sugar mill. Additionally, the payback period of the system can be shortened to 5.79 years.
(3) Through multi-objective optimization, the optimal operating parameters of the system are obtained. The *LCOE* at the optimum working condition is as low as 0.0406$/kWh, and the exergy efficiency is 31.57%. The annual revenue from electricity sales and the saving cost for cooling are $136,300 and $308,600, respectively.
(4) ORC and ARC were used for waste heat gradient utilization from boiler exhaust gas. The system has achieved multi-forms conversion of energy to cooling and generating electricity through cascade utilization of waste heat.
(5) The highest exergy destruction occurs in the generator, accounting for 50.8% of the overall system.

To expand this research in the future, it is necessary to evaluate the system by combining environmental factors. Second, it is crucial to consider the optimization of the heat exchanger model. There are various working fluids that can be used in absorption refrigeration cycles, and it is possible to conduct thermodynamic analysis by switching between them to optimize the system. In addition, it is essential to study different refrigeration systems and thus achieving a more efficient energy conversion system.

Data availability statement

The original contributions presented in the study are included in the article/Supplementary Material, further inquiries can be directed to the corresponding author.

Author contributions

ZW: Writing–original draft, Writing–review and editing. WG: Writing–review and editing. SZ: Methodology, Writing–review and editing. HS: Methodology, Writing–review and editing. WQ: Supervision, Writing–review and editing. LL: Project administration, Writing–review and editing.

Funding

The author(s) declare financial support was received for the research, authorship, and/or publication of this article. This research was supported by Natural Science Foundation of China, (No. 22302044), Science and Technology Major Project of Guangxi under Grant, (AA23062041) and Supported by the Dean/Open Project of Guangxi Key Laboratory of Petrochemical Resource Processing and Process Intensification Technology, (No. 2022K010).

Conflict of interest

Authors SZ and HS were employed by Guangxi Yuchai Machinery Co., Ltd.

The remaining authors declare that the research was conducted in the absence of any commercial or financial relationships that could be construed as a potential conflict of interest.

Publisher's note

All claims expressed in this article are solely those of the authors and do not necessarily represent those of their affiliated organizations, or those of the publisher, the editors and the reviewers. Any product that may be evaluated in this article, or claim that may be made by its manufacturer, is not guaranteed or endorsed by the publisher.

References

Aman, J., Ting, D. S.-K., and Henshaw, P. (2014). Residential solar air conditioning: energy and exergy analyses of an ammonia–water absorption cooling system. *Appl. Therm. Eng.* 62, 424–432. doi:10.1016/j.applthermaleng.2013.10.006

Bandgar, R. S., Jagtap, K. M., Kokare, S. S., and Kshirsagar, A. S. (2018). Waste heat from sugar indusrty to drive vapour absorption acs. *JournalNX* 29 (7), 1039–1051.

Bhattacharyya, S. C., and Quoc Thang, D. N. (2004). Economic buy-back rates for electricity from cogeneration: case of sugar industry in Vietnam. *Energy* 29, 1039–1051. doi:10.1016/j.energy.2003.04.001

Birru, E., Erlich, C., Beyene, G. B., and Martin, A. (2016). Upgrading of a traditional sugar cane mill to a modern mill and assessing the potential of energy saving during steady state and transient conditions—part II: models for a modified cogeneration unit. *Biomass Conv. bioref.* 6, 233–245. doi:10.1007/s13399-015-0180-8

Boukelia, T. E., Arslan, O., and Mecibah, M. S. (2016). ANN-based optimization of a parabolic trough solar thermal power plant. *Appl. Therm. Eng.* 107, 1210–1218. doi:10.1016/j.applthermaleng.2016.07.084

Cai, D., Jiang, J., He, G., Li, K., Niu, L., and Xiao, R. (2016). Experimental evaluation on thermal performance of an air-cooled absorption refrigeration cycle with NH3–LiNO3 and NH3–NaSCN refrigerant solutions. *Energy Convers. Manag.* 120, 32–43. doi:10.1016/j.enconman.2016.04.089

Chouhan, P., and Chandrakar, A. (2014). Performance enhancement of sugar mill by alternate cooling system for condenser. *IOSR J. Mech. Civ. Eng.* 11, 18–25. doi:10.9790/1684-11511825

de Matos, M., Santos, F., and Eichler, P. (2020). "Chapter 1 - sugarcane world scenario," in *Sugarcane biorefinery, technology and perspectives*. Editors F. Santos, S. C. Rabelo, M. De Matos, and P. Eichler (Academic Press), Cambridge, MA, USA, 1–19. doi:10.1016/B978-0-12-814236-3.00001-9

Dogbe, E. S., Mandegari, M., and Görgens, J. F. (2019). Assessment of the thermodynamic performance improvement of a typical sugar mill through the integration of waste-heat recovery technologies. *Appl. Therm. Eng.* 158, 113768. doi:10.1016/j.applthermaleng.2019.113768

Dogbe, E. S., Mandegari, M. A., and Görgens, J. F. (2018). Exergetic diagnosis and performance analysis of a typical sugar mill based on Aspen Plus® simulation of the process. *Energy* 145, 614–625. doi:10.1016/j.energy.2017.12.134

Du, S., Wang, R. Z., and Xia, Z. Z. (2014). Optimal ammonia water absorption refrigeration cycle with maximum internal heat recovery derived from pinch technology. *Energy* 68, 862–869. doi:10.1016/j.energy.2014.02.065

Ebrahimi-Moghadam, A., Farzaneh-Gord, M., Jabari Moghadam, A., Abu-Hamdeh, N. H., Lasemi, M. A., Arabkoohsar, A., et al. (2021). Design and multi-criteria optimisation of a trigeneration district energy system based on gas turbine, Kalina, and ejector cycles: exergoeconomic and exergoenvironmental evaluation. *Energy Convers. Manag.* 227, 113581. doi:10.1016/j.enconman.2020.113581

Fujii, S., Horie, N., Nakaibayashi, K., Kanematsu, Y., Kikuchi, Y., and Nakagaki, T. (2019). Design of zeolite boiler in thermochemical energy storage and transport system utilizing unused heat from sugar mill. *Appl. Energy* 238, 561–571. doi:10.1016/j.apenergy.2019.01.104

Ghannadzadeh, A., and Sadeqzadeh, M. (2017). Exergy aided pinch analysis to enhance energy integration towards environmental sustainability in a chlorine-caustic soda production process. *Appl. Therm. Eng.* 125, 1518–1529. doi:10.1016/j.applthermaleng.2017.07.052

Hung, T. C., Shai, T. Y., and Wang, S. K. (1997). A review of organic rankine cycles (ORCs) for the recovery of low-grade waste heat. *Energy* 22, 661–667. doi:10.1016/S0360-5442(96)00165-X

Kapanji, K. K., Haigh, K. F., and Görgens, J. F. (2021). Techno-economics of lignocellulose biorefineries at South African sugar mills using the biofine process to co-produce levulinic acid, furfural and electricity along with gamma valeractone. *Biomass Bioenergy* 146, 106008. doi:10.1016/j.biombioe.2021.106008

Khaljani, M., Khoshbakhti Saray, R., and Bahlouli, K. (2015). Comprehensive analysis of energy, exergy and exergo-economic of cogeneration of heat and power in a combined gas turbine and organic Rankine cycle. *Energy Convers. Manag.* 97, 154–165. doi:10.1016/j.enconman.2015.02.067

Kumar, B., Selvarasan, I., Annadurai, G., and Ramalingam, S. (2018). Thermodynamic analysis of a single effect lithium bromide water absorption system using waste heat in sugar industry. *Therm. Sci.* 22, 507–517. doi:10.2298/tsci151013285b

Li, T. X., Wang, R. Z., Kiplagat, J. K., Wang, L. W., and Oliveira, R. G. (2009). Thermodynamic study of a combined double-way solid–gas thermochemical sorption refrigeration cycle. *Int. J. Refrig.* 32, 1570–1578. doi:10.1016/j.ijrefrig.2009.05.004

Li, T. X., Wang, R. Z., and Li, H. (2014). Progress in the development of solid–gas sorption refrigeration thermodynamic cycle driven by low-grade thermal energy. *Prog. Energy Combust. Sci.* 40, 1–58. doi:10.1016/j.pecs.2013.09.002

Li, T. X., Xu, J. X., Yan, T., and Wang, R. Z. (2016). Development of sorption thermal battery for low-grade waste heat recovery and combined cold and heat energy storage. *Energy* 107, 347–359. doi:10.1016/j.energy.2016.03.126

Li, X., Song, J., Yu, G., Liang, Y., Tian, H., Shu, G., et al. (2019). Organic Rankine cycle systems for engine waste-heat recovery: heat exchanger design in space-constrained applications. *Energy Convers. Manag.* 199, 111968. doi:10.1016/j.enconman.2019.111968

Liu, X., Yang, X., Yu, M., Zhang, W., Wang, Y., Cui, P., et al. (2020). Energy, exergy, economic and environmental (4E) analysis of an integrated process combining CO2 capture and storage, an organic Rankine cycle and an absorption refrigeration cycle. *Energy Convers. Manag.* 210, 112738. doi:10.1016/j.enconman.2020.112738

Lu, F., Zhu, Y., Pan, M., Li, C., Yin, J., and Huang, F. (2020). Thermodynamic, economic, and environmental analysis of new combined power and space cooling system for waste heat recovery in waste-to-energy plant. *Energy Convers. Manag.* 226, 113511. doi:10.1016/j.enconman.2020.113511

Luo, D., Mahmoud, A., and Cogswell, F. (2015). Evaluation of low-GWP fluids for power generation with organic rankine cycle. *Energy* 85, 481–488. doi:10.1016/j.energy.2015.03.109

Malwe, P. D., Gawali, B. S., Choudhari, M. S., Dhalait, R. S., and Deshmukh, N. S. (2021). Energy and exergy analysis of an organic rankine cycle integrated with vapour compression refrigeration system. *Adv. Appl. Math. Sci.* 20.

Mana, A. A., Kaitouni, S. I., Kousksou, T., and Jamil, A. (2023). Enhancing sustainable energy conversion: comparative study of superheated and recuperative ORC systems for waste heat recovery and geothermal applications, with focus on 4E performance. *Energy* 284, 128654. doi:10.1016/j.energy.2023.128654

Men, Y., Liu, X., and Zhang, T. (2021). Performance comparison of different total heat exchangers applied for waste heat recovery. *Appl. Therm. Eng.* 182, 115715. doi:10.1016/j.applthermaleng.2020.115715

Mohammadi, F., Roedl, A., Abdoli, M. A., Amidpour, M., and Vahidi, H. (2020). Life cycle assessment (LCA) of the energetic use of bagasse in Iranian sugar industry. *Renew. Energy* 145, 1870–1882. doi:10.1016/j.renene.2019.06.023

Nami, H., and Anvari-Moghaddam, A. (2020). Small-scale CCHP systems for waste heat recovery from cement plants: thermodynamic, sustainability and economic implications. *Energy* 192, 116634. doi:10.1016/j.energy.2019.116634

Nami, H., Arabkoohsar, A., and Anvari-Moghaddam, A. (2019). Thermodynamic and sustainability analysis of a municipal waste-driven combined cooling, heating and power (CCHP) plant. *Energy Convers. Manag.* 201, 112158. doi:10.1016/j.enconman.2019.112158

Nami, H., Nemati, A., and Jabbari Fard, F. (2017). Conventional and advanced exergy analyses of a geothermal driven dual fluid organic Rankine cycle (ORC). *Appl. Therm. Eng.* 122, 59–70. doi:10.1016/j.applthermaleng.2017.05.011

Nemati, A., Nami, H., Ranjbar, F., and Yari, M. (2017). A comparative thermodynamic analysis of ORC and Kalina cycles for waste heat recovery: a case study for CGAM cogeneration system. *Case Stud. Therm. Eng.* 9, 1–13. doi:10.1016/j.csite.2016.11.003

Nemomsa, S., Tibba, G., Dejene, N., and Negeri, D. (2022). *Design and simulation of combined flue gas and steam bagasse dryer to increase boiler efficiency of sugar factory*. Rochester, NY, USA: Social Science Research Network. doi:10.2139/ssrn.4064539

Pan, M., Lu, F., Zhu, Y., Li, H., Yin, J., Liao, Y., et al. (2021). 4E analysis and multiple objective optimizations of a cascade waste heat recovery system for waste-to-energy plant. *Energy Convers. Manag.* 230, 113765. doi:10.1016/j.enconman.2020.113765

Pan, M., Zhu, Y., Liang, Y., Lu, F., Zhi, R., and Xiao, G. (2021). Performance assessment of a waste-heat driven CO2-based combined power and refrigeration cycle for dual-temperature refrigerated truck application. *Energy Convers. Manag.* 249, 114863. doi:10.1016/j.enconman.2021.114863

Pethurajan, V., Sivan, S., and Joy, G. C. (2018). Issues, comparisons, turbine selections and applications – an overview in organic Rankine cycle. *Energy Convers. Manag.* 166, 474–488. doi:10.1016/j.enconman.2018.04.058

Rosillo-Calle, F. (2016). A review of biomass energy – shortcomings and concerns. *J. Chem. Technol. Biotechnol.* 91, 1933–1945. doi:10.1002/jctb.4918

Singh, O. K. (2019). Exergy analysis of a grid-connected bagasse-based cogeneration plant of sugar factory and exhaust heat utilization for running a cold storage. *Renew. Energy* 143, 149–163. doi:10.1016/j.renene.2019.05.012

Singh, O. K. (2020). Application of Kalina cycle for augmenting performance of bagasse-fired cogeneration plant of sugar industry. *Fuel* 267, 117176. doi:10.1016/j.fuel.2020.117176

Srikhirin, P., Aphornratana, S., and Chungpaibulpatana, S. (2001). A review of absorption refrigeration technologies. *Renew. Sustain. Energy Rev.* 5, 343–372. doi:10.1016/S1364-0321(01)00003-X

Tan, D., Wu, Y., Lv, J., Li, J., Ou, X., Meng, Y., et al. (2023). Performance optimization of a diesel engine fueled with hydrogen/biodiesel with water addition based on the response surface methodology. *Energy* 263, 125869. doi:10.1016/j.energy.2022.125869

The Chemical Engineering Plant Cost Index (n.d.), (2022). Chemical Engineering. Available at: https://www.chemengonline.com/pci-home/ (Accessed September 21, 2022).

Tian, M., Yu, Z., Zhao, H., and Yin, J. (2018). Thermodynamic analysis of an integrated solid oxide fuel cell, Organic Rankine Cycle and absorption chiller trigeneration system with CO2 capture. *Energy Convers. Manag.* 171, 350–360. doi:10.1016/j.enconman.2018.05.108

Uphade, D. B. (2021). The potential of heat recovery for air-conditioning in sugar industry. *J. Inst. Eng. India Ser. C* 102, 1299–1309. doi:10.1007/s40032-021-00741-4

Usda, U. S. D. of A, (2018). *Sugar: world markets and trade*. USDA. Washington, DC, USA.

Vaja, I., and Gambarotta, A. (2010). Internal combustion engine (ICE) bottoming with organic rankine cycles (ORCs). *Energy* 35, 1084–1093. doi:10.1016/j.energy.2009.06.001

Wang, S., Liu, C., Li, J., Sun, Z., Chen, X., and Wang, X. (2020). Exergoeconomic analysis of a novel trigeneration system containing supercritical CO2 Brayton cycle, organic Rankine cycle and absorption refrigeration cycle for gas turbine waste heat recovery. *Energy Convers. Manag.* 221, 113064. doi:10.1016/j.enconman.2020.113064

Wang, X.-Q., Li, X.-P., Li, Y.-R., and Wu, C.-M. (2015). Payback period estimation and parameter optimization of subcritical organic Rankine cycle system for waste heat recovery. *Energy* 88, 734–745. doi:10.1016/j.energy.2015.05.095

Zare, V. (2020). Performance improvement of biomass-fueled closed cycle gas turbine via compressor inlet cooling using absorption refrigeration; thermoeconomic analysis and multi-objective optimization. *Energy Convers. Manag.* 215, 112946. doi:10.1016/j.enconman.2020.112946

Zhang, H., Liu, Y., Liu, X., and Duan, C. (2020). Energy and exergy analysis of a new cogeneration system based on an organic Rankine cycle and absorption heat pump in the coal-fired power plant. *Energy Convers. Manag.* 223, 113293. doi:10.1016/j.enconman.2020.113293

Zhang, X., Liu, X., Sun, X., Jiang, C., Li, H., Song, Q., et al. (2018). Thermodynamic and economic assessment of a novel CCHP integrated system taking biomass, natural gas and geothermal energy as co-feeds. *Energy Convers. Manag.* 172, 105–118. doi:10.1016/j.enconman.2018.07.002

Zhang, X., Wu, L., Wang, X., and Ju, G. (2016). Comparative study of waste heat steam SRC, ORC and S-ORC power generation systems in medium-low temperature. *Appl. Therm. Eng.* 106, 1427–1439. doi:10.1016/j.applthermaleng.2016.06.108

Nomenclature

Abbreviation

A	heat transfer area (m^2)
P	Pressure (MPa)
T	temperature (K)
U	overall heat transfer coefficient ($W/(m^2{\cdot}K)$)
Z	capital cost of a component ($)
$\dot{Z}$	capital cost rate ($/h)
h	enthalpy (kJ/kg)
s	entropy (kJ/(kg·K))
V	Volume (m^3)
$\dot{I}$	exergy loss (kJ)
$\dot{E}$	exergy rate (kW)
$\dot{Q}$	heat transfer rate (kW)
p_e	price of electricity ($/kWh)
$\dot{W}$	power (kW)
$\dot{m}$	mass flow rate (kg/s)
$\dot{H}$	enthalpy rate (kW)

Abbreviations

ARC	Absorption refrigeration cycle
Abs	Absorber
AWM	Ammonia-Water Mixture
COP	Coefficient of performance
CRF	Capital recovery factor
PP	Payback period (year)
NE	Net earning per year ($/year)
Cond	Condenser
Eva	Evaporator
Gen	Generator
HE	Heat Exchanger
LCOE	Levelized Cost of Energy
ODP	ODP Ozone Depletion Potential
ORC	Organic Rankine Cycle
SHE	Solution heat exchanger
Thv	Throttle valve
ORCT	Turbine

Subscripts

0	environment
01–16	state points
a1	cooling water inlet of absorber
a2	cooling water outlet of absorber
c1	cooling water inlet of condenser 2
c2	cooling water outlet of condenser 2
ei	inlet of the evaporator
eo	outlet of the evaporator
go	inlet of flue gas
gin	outlet of flue gas in HE
gout	final state of flue gas
P1	Pump1
P2	Pump2
Ex	exergy
in	inlet
net	net power
out	outlet
OM	operating and maintenance
cw	cooling water
Q	Heat
D	destruction
e	Exit
f	fuel
g	gas
p	production

Greek letters

η	efficiency (%)
ΔT	temperature difference (K)
ΔT_{LMTD}	log mean temperature difference (K)